2022, pp. 1–6

UCF

doi: DOI HERE
Advance Access Publication Date: Day Month Year
Paper

PAPER

A study of the Growth of Pb clusters on Ge(111) and Ge(100)

Theodoros E. Panagiotakopoulos, Duy Le and Talat S. Rahman

Department of Physics, University of Central Florida, 4111 Libra Drive, 32816, Orlando, Florida, USA

Abstract

Formation of nanoclusters is a hot topic of research in either experimental and theoretical research. In this article, we study the details of the Pb growth clusters on Ge (111) and Ge (100) respectively. In detail, we have performed ab initio density-functional calculations of total energies for Pb/Ge(111), Ge(100) and Pb/Ge(100) by calculating the Pb's chemical Potential as a function of Pb coverage. In the case of Pb/Ge(111), we have found that the formation of Pb clusters start at 1.33 ML coverage. As far as Ge(100) is concerned, we find that p(2x2) and c(4x2) are the lowest-energy reconstructions and are nearly degenerate in energy while we also explain this result. Furthermore, the formation of Pb islands on Ge(100) surface is found to take place at around 1.56 ML coverage.

Key words: Ge(100), Ge(111), chemical potential, Pb clusters, Density Functional Theory

Introduction

A crucial technological process is the formation of single crystal metal islands on semiconductor surfaces. The study of the epitaxial growth of metal on semiconductor surface is used in the manufacture of raw-materials into finished goods and also in industry. With continued downscaling of semiconductor devices, a transition from the current micrometer-scale fabrication technology to a new nanometer-scale fabrication technology will occur. A thorough understanding of the physical characteristics of nanometer size systems is required for successful nanofabrication methods. The capability to easily construct nanoscale scale structures is critical for future nanotechnology advancements.

When utilized to define nanoscale features, direct usage of standard lithographic techniques like electron beam lithography or scanning probe microscope related nanolithography [1] becomes slow. Self-assembly techniques have recently piqued interest for nanoscale device applications because they allow for the fabrication of nanoscale elements such as quantum dots and electrical device configurations of these nanoscale elements without the usage of traditional lithographic procedures. [2] [3] [4] [5]. The usage of pre-formed nanoscale metallic clusters is a recurrent theme in these self-assembly protocols. [6]

At this time, it's difficult to say with any certainty what final electronic functionality nanoparticles will provide. Nanoscale crystalline clusters' small size and regular geometric shape will probably certainly be exploited in prototype designs of simple electronic circuits comparable to those already utilized in practice in the near future. In the long run, forming cluster networks on active semiconductor surfaces to offer periodic lateral modulation of the underlying substrate's electrical characteristics appears potential. Patterning accomplished through cluster self-assembly might be translated onto the substrate via selective etching with the clusters as an etch mask or generated by electrical interactions at the cluster-substrate interface.[6] The potential to give low-cost design flexibility to a cluster network by functionalizing it with any connecting molecules of choice is appealing. Advanced computing, biological, and chemical sensing applications can benefit from tailoring the lateral electron transport in a cluster network positioned between two or more contact pads, as well as the vertical electron transport into a semiconducting substrate. There have already been scenarios presented for achieving practical electronic functioning in cluster-based devices.[7]

Semiconductor substrates are of special importance in this context because they appear to give the most direct approach to useful electronic functionality at this time. Single electron tunneling (SET) devices, nanoscale Schottky barriers [7], and nanoscale ohmic contacts are the three broad categories of published work. Scanning probe microscopy is used extensively in almost all of the published work. Another significant

challenge is the precise placement of metallic clusters on semiconductors.

While a number of papers have highlighted some of the recent work in this field that shows promise, such as the ability to push and locate clusters using scanning probe tips, few research have been documented that provide a comprehensive solution to the essential challenge of accurate cluster positioning. In what follows, we'll look at some recent research that shows promise in this area.

This study presents the results of an ab initio theoretical investigation of the energetics for Pb on unreconstructed Ge(111) surface, and makes use of chemical potential to calculate the coverage at which Pb islands are observed on the Ge(111) surface. Moreover, the results of an ab initio theoretical examination of the energetics for one family of dimer reconstructions of the Ge(100) surface are presented in this paper. In the three sections that follow, we (1) describe the calculational process we employed, (2) describe our results in relation to experiments, and (3) present our conclusions.

Computational Details

Total energy calculations were performed using VASP [8], employing the projector-augmented wave [9] [10] and the plane-wave basis set and energy cutoffs of 500 eV and the slab was sampled using 3 × 3 × 1 k-point grid scheme for relaxation and 1 x 1 x 1 for energy calculations. The Pb/Ge(1 1 1) and Pb/Ge(100) systems were modeled by repeated asymmetric slab consisting of ten Ge layers with Pb monolayer on the top side of the slab. The optimized bulk Ge lattice constant of 5.647$\mathring{A}$ (experimental value for bulk Ge is 5.64$\mathring{A}$ [11]) and a spatial spacing between the slabs of 15$\mathring{A}$ were used in all calculations. The Hubbard U value is set to 2.94 eV since this number gives the 0.67 eV band gap for Ge. **Sheram paper**

We will use the definiton of chemical potential in order to interprete our data. We have to recallthat in thermodynamics, chemical potential of a species is energy that can be absorbed or releaseddue to a change of the particle number of the given species. The samller the chemical potential is, the easier is to add an atom in our system.

$$\mu = \left(\frac{\partial U}{\partial N}\right)_{S,V} \tag{1}$$

Moving from continues to discrete, the chemical potential used for our calculations is given by the following formula:

$$\mu^{c}_{Pb} = \frac{E^{c}_{Pb/Ge(111)} - E^{c-\delta c}_{Pb/Ge(111)}}{\delta N_{Pb}} \tag{2}$$

where c means coverage. $E^{c}_{Pb/Ge(111)}$ is the energy of a configuration at certain coverage c, $E^{c-\delta c}_{Pb/Ge(111)}$) is the energy at a configuration with coverage δc and δN_{Pb} is the change in the number of Pb atoms.

For either Pb/Ge(100) and Pb/Ge(111), we performed DFT calculations for Pb atoms, from 1 ML to 1.69 ML on Ge(111) and from 1 ML to 2 ML coverage for Pb/Ge(100), by forcing Pb atoms to be in a single layer. This means that we do not allow them to form second layer. For each coverage, we calculate the average chemical potential of Pb atoms that comes from 5 different structures.

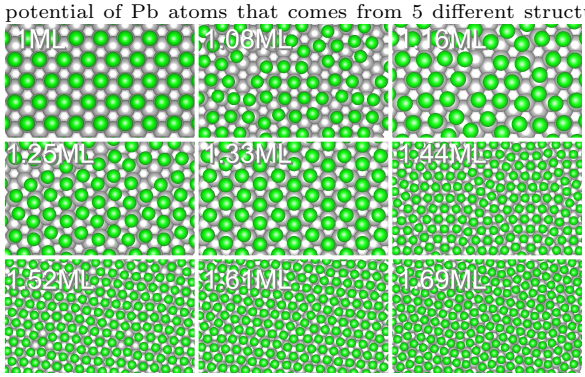

Fig. 1. Pb/Ge(111) top view for different coverages

For Ge(100) surface atoms are being reconstracted in order to form dimers and reduce the total energy of the system[12]. The total energy of the four members of the (2x1) family of buckled dimer reconstructions was computed and minimized. As seen in Figures 4, 5, 6, 7, the (2x1) family is defined by rows of dimers. The members differ in the arrangement of "up" and "down" dimers in and perpendicular to the dimer rows on the (2X1) backbone. An tenlayer slab and c(4x2) unit cell , a vacuum zone of 9.8 $\mathring{A}$, and periodic boundary conditions in all directions were used to describe the surface. All of the atoms were free to move, however we could get the same relults if the innermost two layers were frozen[13]. To accurately compare the total energies of the various symmetry reconstructions in terms of basis functions and k points, we performed all calculations in a (4x2) unit cell while maintaining either precise b(2x1), (4x1), c(4x2), or p(2x2) symmetry within this supercell. As a result, we used a unit cell of 80 atoms and a volume of 126 atomic volumes in our calculations.

Results

Pb/Ge(111)

For a single Pb atom on a 6x6 super cell the most favorable geometry is found to be T4, as we can see from the table bellow:

Table 1. Summary of the energy of the estimated geometries at low coverage, with respect to H3

System	Δenergy (eV)
1. H3	0
2. T1	0.033
2. T4	-0.082

The average Pb-Ge bond length was found to be 2.949$\mathring{A}$ **charge difference plott supplement**

For the 1/3 ML coverage, the so called α phase, Pb atoms adsorbed at T4 sites of the Ge(111) substrate, which is in agreement with theoretical results.

Table 2. Summary of the energy of the estimated geometries, with respect to T1 for 1/3 ML coverage

System	Δenergy (eV)
1. H3	0
2. T1	1.139
3. T4	-0.267

The average bond length between Pb and Ge atoms, is found to be 2.961 $\AA$ and Pb is bonding with four Ge atoms. For 1 ML coverage, geometry T1 was discovered to be the most energetically favorable, which agrees with theoretical predictions[14] and experiments [15]. T1 has a lower energy than geometries H3 and T4 by 0.41 and 0.48 eV, respectively.

Table 3. Summary of the energy of the estimated geometries, with respect to T1 for 1 ML coverage

System	Δenergy (eV)
1. H3	0.41
2. T1	0
3. T4	0.48

Further insights are obtained from ab initio thermodynamic calculations which confirm that at Pb coverages below 1.33 ML the chemical potential of Pb in the wetting layer is less than that in bulk Pb, suggesting that Pb atoms prefer to be in the wetting layer, while at coverages higher than 1.33 ML the order is reversed implying that Pb atoms prefer to form bulk crystal, i.e. cluster. More interestingly, we find that at above 1.33 ML coverage, the chemical potential of Pb bilayer on Ge(111) is higher than that in bulk Pb, alluding that Pb atoms prefers to form a cluster, not a bilayer, in agreement with the LEEM observations

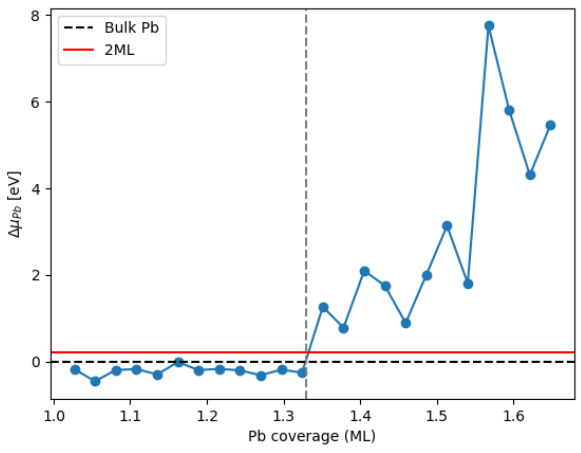

Fig. 2. $\Delta\mu_{Pb} = \mu_{Pb} - \mu_{Pbbulk}$ vs Pb coverage. μ_{Pb} is the average chemical potential of Pb at certain coverage that comes from five different structures where Pb was moved arbitrary in five different directions by 1$\AA$ in order to get a smoother behavior. μ_{Pbbulk} is the lead's bulk chemical potential

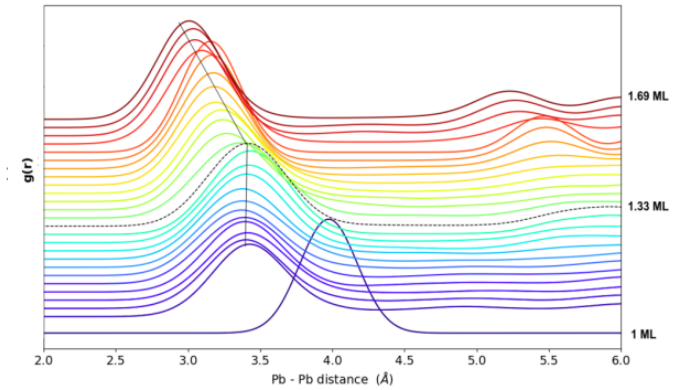

Fig. 3. Radial distribution functuion for Pb atoms placed on Ge(111) surface

Lower than 1.33 ML coverage, there is no compression in the nearest neighbor distance. But above the 1.33 ML coverage there is compression. This explains, the positive at Pb coverage higher than 4/3 ML and experimental observation that islands start to form after a 4/3 ML.

Ge(100)

Ge(100) surface atoms are being reconstracted in order to form dimers and reduce the total energy of the system[12]. The total energy of the four members of the (2x1) family of buckled dimer reconstructions was computed and minimized. The (2x1) family is defined by rows of dimers. [13]. The members differ in the arrangement of "up" and "down" dimers in and perpendicular to the dimer rows on the (2X1) backbone. An tenlayer slab and c(4×2) unit cell , a vacuum zone of 9.8 $\AA$, and periodic boundary conditions in all directions were used to describe the surface. All of the atoms were free to move, however we could get the same relults if the innermost two layers were frozen[13]. To accurately compare the total energies of the various symmetry reconstructions in terms of basis functions and k points, we performed all calculations in a (4x2) unit cell while maintaining either precise b(2×1), (4×1), c(4×2), or p(2×2) symmetry within this supercell.
The total energy per dimer for the b(2×1), p(4×1), c(4×2), and energy p(2×2) symmetry configurations are listed in Table I, with the energy of the b(2x1) symmetry regarded as the energy zero.

Table 4. Total energy of (2×1) family configurations.

System	Δenergy (eV)
1. b(2×1)	0
2. p(4×1)	0.033
3. p(2×2)	-0.082
4. c(4×2)	-0.083

The discrcmepancy of a few meV/dimer between the p(2×2) and c(4×2) symmetry reconstructions is within calculation errors. Kubby's [16] and Lambert's [17] conclusion that the p (2 × 2) configuration is essentially degenerate with the c(4×2) configuration is correct. At room temperature, they found both p(2×2) and c(4×2) systems coexisting with b(2×1) on the (100) surface, using STM. However, this contradicts Culbertson, Yuk, and Feldman's findings [18], which only report c(4X2)

diffraction patterns at low temperatures. Because of Ihm et al's [19] tight-binding work on Si and previous ab initio work on Ge by Jannopoulo's [13], I expected p(2×2) and c(4×2) to have similar energies.
The relaxation of the atoms in the layer below the dimers is responsible for the decrease in surface energy when the buckling direction alternates from dimer to dimer along a column. The atoms in this layer move towards the raised dimer atom and away from the lowered dimer atom in the c(4×2) and p(2×2) reconstructions. Atoms also move in planes perpendicular to the arrows, but only the relaxation in the arrows' direction distinguishes the high- and low-energy reconstructions. The atoms' relaxation in the directions depicted in figure 5 keeps the lengths of the bonds between the dimer atoms and the first-layer atoms near to the bulk bond length, resulting in very minimal stretching of the first-layer atoms and the dimers.

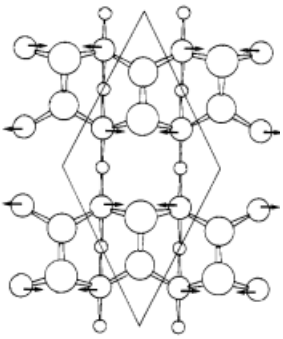

[20]

Fig. 4. c(4×2) reconstruction on Ge (001). The arrows show the relaxation of the atoms in the first layer that stabilises alternation in the dimer buckling direction down the columns.

After finding the most stable configuration of Ge(100), p(2x2).

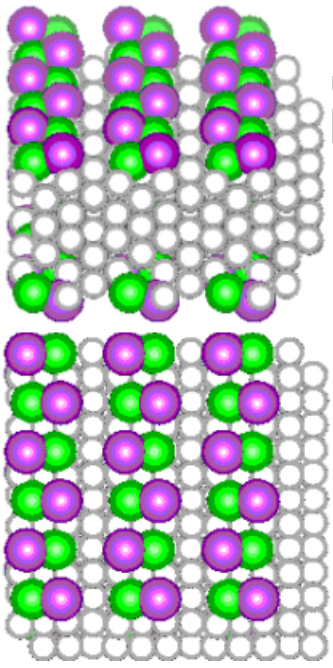

Fig. 5. Centered 2x2 symmetry configuration, Purple: top dimer atoms, green: down dimer atoms

Pb/Ge(100)

We continue by adsorbing a single Pb adatom on it in order to find the most favorable absorption site. We have only two possible adsorption sites, known as H and M.[21]

Table 5. Total energy of Pb/Ge(100), where Pb adatoms are placed on H and M sites

System	Δenergy (eV)
1. H	0
2. M	-0.14

We get that the most favorable site of Pb on Ge(100) is M, in agreement with similar works [22]
We computed and minimized the total energy of the two members of the (2×1) family of buckled dimer reconstructions, the c(4×2) and p(2×2), with 1 ML coverage of Pb. The c(4×2) and p(2×2) systems are found to have the lowest and almost the same energy. Eight different systems of Pb/Ge(100) with 1 ML coverage, were used to figure out which surface we would use to start absorbing lead atoms on. More specificaly, all the systems consist of 192 atoms in total, 32 Pb on the surface and 160 Ge.

Table 6. Summary of the energy of the used geometries.

System	p(2x2) (eV)	c(4x2) (eV)
1.	-1040.77	-1400.61
2.	-1041.83	-1040.26
3.	-1041.49	-1039.81
4.	-1041.49	-1040.14

From the table above it is seen that from the considered geometries, p(2×2) have less energy so they are more stable.
Germanium atoms are arranged on ten layers, a vacuum zone of 9.8$\mathring{A}$, and periodic boundary conditions in all directions were used to describe all the eight systems.
Starting with the second system of the Table 6, p(2x2) with energy -1041.83 eV. The total energy for the two site configurations M and H are listed in Table bellow, with the energy of H regarded as the energy zero.
It is found that for the lowest energy configurations (M site), one Pb atom bonds with three Ge atoms, with an average bond length 2.88 $\mathring{A}$.

Moreover, ab initio thermodynamic calculations confirm that the chemical potential of Pb in the wetting layer is less than that of bulk Pb at Pb coverages below 1.59 ML, implying that Pb atoms prefer to be in the wetting layer, whereas at coverages higher than 1.59 ML, the order is reversed, implying that Pb atoms prefer to form bulk crystal, i.e. cluster. More intriguingly, we discover that the chemical potential of a Pb bilayer on Ge(111) is higher than that of bulk Pb at 1.59 ML coverage, implying that Pb atoms prefer to form a cluster rather than a bilayer.

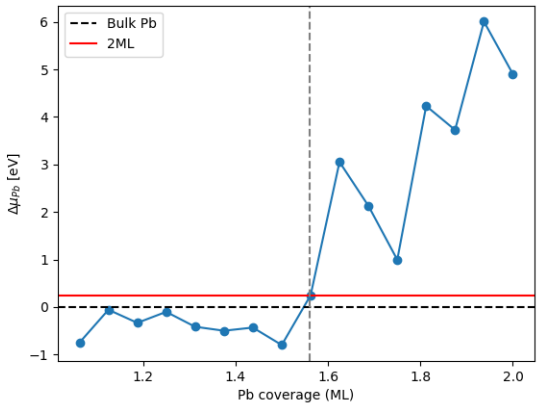

Fig. 6. $\Delta\mu_{Pb} = \mu_{Pb} - \mu_{Pbbulk}$ vs Pb coverage. μ_{Pb} is the average chemical potential of Pb at certain coverage that comes from five different structures where Pb was moved arbitrary in five different directions by $1\mathring{A}$ in order to get a smoother behavior. μ_{Pbbulk} is the lead's bulk chemical potential

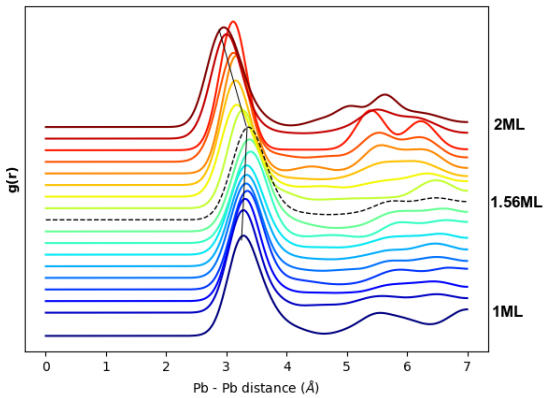

Fig. 7. Radial distribution functuion for Pb atoms placed on Ge(100) surface

Lower than 1.56 ML coverage, there is no compression in the nearest neighbor distance. But above the 1.56 ML coverage there is compression. This explains, the positive at Pb coverage higher than 1.56 ML.

Conclusion

Pb/Ge(111)

Finally, we get that the formation of Pb islands starts at around 1.33 ML coverage as it can be seen from either the radial distribution function and from the chemial potential vs Pb's coverage

Ge(100)

By altering the buckling orientations of the dimers, an unlimited number of reconstructions can be built on this surface, and any finite number of calculations for the surface energy of alternative arrangements of buckled dimers cannot establish which is the most stable surface reconstruction. The b(2x1), c(4x2), p(2x2), and p(4×1) configurations were chosen for our computations. Table 1 shows the surface energy per dimer for these buckling dimer configurations. The c(4×2) and p(2×2) reconstructions, in which the buckling direction alternates from dimer to dimer down the columns, have lower energy than the b(2x1) and p(4x1) reconstructions, in which the buckling direction is the same.

Pb/Ge(100)

Finally, we get that the formation of Pb islands starts at around 1.5l ML coverage as it can be seen from either the radial distribution function and from the chemial potential vs Pb's coverage

Funding

Funding Acknowledgment: NSF DMR-1701748, NSF DMR-1710306, USDOE DE-AC02-07CH11358

References

1. Pengfei Fan, Jian Gao, Hui Mao, Yanquan Geng, Yongda Yan, Yuzhang Wang, Saurav Goel, and Xichun Luo. Scanning probe lithography: state-of-the-art and future perspectives. *Micromachines*, 13(2):228, 2022.
2. B Amir Parviz, Declan Ryan, and George M Whitesides. Using self-assembly for the fabrication of nano-scale electronic and photonic devices. *IEEE transactions on advanced packaging*, 26(3):233–241, 2003.
3. Michael A Boles, Michael Engel, and Dmitri V Talapin. Self-assembly of colloidal nanocrystals: From intricate structures to functional materials. *Chemical reviews*, 116(18):11220–11289, 2016.
4. Eberechukwu Victoria Amadi, Anusha Venkataraman, and Chris Papadopoulos. Nanoscale self-assembly: concepts, applications and challenges. *Nanotechnology*, 2021.
5. Jia Liu, Takhee Lee, DB Janes, BL Walsh, MR Melloch, JM Woodall, R Reifenberger, and RP Andres. Guided self-assembly of au nanocluster arrays electronically coupled to semiconductor device layers. *Applied Physics Letters*, 77(3):373–375, 2000.
6. Takhee Lee, Jia Liu, Nien-Po Chen, RP Andres, DB Janes, and R Reifenberger. Electronic properties of metallic nanoclusters on semiconductor surfaces: Implications for nanoelectronic device applications. *Journal of Nanoparticle Research*, 2(4):345–362, 2000.
7. Debashis Panda, Paritosh Piyush Sahu, and Tseung Yuen Tseng. A collective study on modeling and simulation of resistive random access memory. *Nanoscale research letters*, 13(1):1–48, 2018.
8. G. Kresse and J. Furthmüller. Efficiency of ab-initio total energy calculations for metals and semiconductors using a plane-wave basis set. *Computational Materials Science*, 6(1):15–50, 1996.
9. P. E. Blöchl. Projector augmented-wave method. *Phys. Rev. B*, 50:17953–17979, Dec 1994.
10. John P. Perdew, Kieron Burke, and Matthias Ernzerhof. Generalized gradient approximation made simple. *Phys. Rev. Lett.*, 77:3865–3868, Oct 1996.
11. Philipp Haas, Fabien Tran, and Peter Blaha. Calculation of the lattice constant of solids with semilocal functionals. *Phys. Rev. B*, 79:085104, Feb 2009.
12. M Needels, MC Payne, and JD Joannopoulos. High-order reconstructions of the ge (100) surface. *Physical Review B*, 38(8):5543, 1988.
13. M Needels, MC Payne, and JD Joannopoulos. Ab initio molecular dynamics on the ge (100) surface. *Physical review letters*, 58(17):1765, 1987.
14. Maciej Szary, Barbara Pieczyrak, Leszek Jurczyszyn, and Marian Radny. Suppressed and enhanced spin polarization in the 1ml-pb/ge(111)-1 × 1 system. *Applied Surface Science*, 466:224–229, 02 2019.
15. Ing-Shouh Hwang and Jene A. Golovchenko. Phase transition of monolayer pb/ge(111). *Phys. Rev. B*, 50:18535–18542, Dec 1994.
16. JA Kubby, JE Griffith, RS Becker, and JS Vickers. Tunneling microscopy of ge (001). *Physical Review B*, 36(11):6079, 1987.
17. WR Lambert, PL Trevor, MJ Cardillo, A Sakai, and DR Hamann. Surface structure of ge (100) studied by he diffraction. *Physical Review B*, 35(15):8055, 1987.
18. RJ Culbertson, Y Kuk, and LC Feldman. Subsurface strain in the ge (001) and ge (111) surfaces and comparison to silicon. *Surface science*, 167(1):127–140, 1986.
19. J Ihm, DH Lee, JD Joannopoulos, and JJ Xiong. Structural phase diagrams for the surface of a solid: a total-energy, renormalization-group approach. *Physical review letters*, 51(20):1872, 1983.
20. MC Payne, M Needels, and JD Joannopoulos. Surface reconstructions on germanium. *Journal of Physics: Condensed Matter*, 1(SB):SB63, 1989.
21. V. Milman, D. E. Jesson, S. J. Pennycook, M. C. Payne, M. H. Lee, and I. Stich. Large-scale ab initio study of the binding and diffusion of a ge adatom on the si(100) surface. *Phys. Rev. B*, 50:2663–2666, Jul 1994.
22. Young-Jo Ko, Kang-Ho Park, Jeong Sook Ha, and Wan Soo Yun. Ab initio study of the mixed dimer formation in ge growth on si(100). *Phys. Rev. B*, 60:8158–8163, Sep 1999.